First-principles evaluation of resistance contributions in Ruthenium interconnects for advanced technology nodes

Hemant Dixit[1] Jin Cho[2] and Francis Benistant[3]

[1]*GLOBALFOUNDRIES, 400 Stone Break Rd Extn, Malta, NY 12020 USA*
[2]*GLOBALFOUNDRIES, 2600 Great America Way, Santa Clara, CA 95054 USA*
[3]*GLOBALFOUNDRIES, 60 Woodlands Industrial Park D Street 2, Singapore 738406*

Abstract— **Resistance contribution within Ruthenium (Ru) interconnects, used in middle-of-the line and back-end-of-the line process in an integrated circuit, are evaluated using first-principles density functional theory based transport calculations using the non-equilibrium Green's function. Three prominent scattering mechanisms - impurity scattering, interface/surface scattering and grain-boundary reflections are studied systematically. The results are compared with available resistivity data from literature. The calculated reflection coefficients (R) for the symmetric-tilt grain boundaries lie in the range of 0.38 to 0.51, indicating the grain boundary reflections can significantly enhance the metal resistivity within Ru interconnects. These grain boundary reflection coefficients are in good agreement with hardware data and a fit to the measured resistivity data predicts an average reflection coefficient of 0.51 for Ru interconnect, using Mayadas-Shatzkes model. The results obtained provide useful physical insights into Ru grain-boundary reflections and can be used to classify the metals for advanced interconnect technology.**

Keywords—Metal interconnect, Via resistivity. Ruthenium, Grain boundary

I. Introduction

DEVELOPMENT of sub-10 nm advanced technology nodes requires a significant reduction in the thickness of the metal wires which connect open transistors, in the middle-of-line (MOL) and back end of the line (BEOL) process, to form an integrated circuit (IC). However, the resistance offered by the metal interconnects increases with decreasing widths. This size effect represents a major challenge for downsizing of IC's and development of sub-10 nm nodes. The primary reason for increasing resistivity is due to enhanced electron scattering at the external surface and at the grain boundaries present within the metal. In this article, we evaluate the scattering mechanism within Ruthenium interconnect using the transport calculations based on the first-principles Density Functional Theory (DFT) and Non-equilibrium Green's Function (NEGF) method.

The search for alternative metals other than Copper (Cu) and Tungsten (W), has led to Ruthenium (Ru) as potential candidate [1]–[4]. Impurity scattering, interface scattering and grain-boundary reflections are primary scattering mechanism within the metal interconnects that contributes to its enhanced resistivity. Typically, presence of impurities which include - foreign atoms and point defects such as self-interstitials and vacancies are known to reduce the electron transmission and increase metal resistivity. Here, we investigate the role of commonly observed impurities such as Carbon (C) and Oxygen (O), owing to the MOL/BEOL process conditions, within the Ru interconnects. Besides foreign impurities, the intrinsic point defects such as - Ru interstitial and Ru vacancy, are also studied. The defect concentrations are chosen to be ~ $2e^{20}/cm^3$ as observed in the experiment [1]. Besides impurity scattering, we also look at the vertical resistance across Ru-liner metal interface and the scattering due to presence of symmetric tilt grain boundaries. This paper is organized as follows. Section II describes the theory and computational details used to evaluate the resistivity in Ru interconnect. Section III, IV and V describes the results obtained for three prominent scattering mechanisms – impurity scattering, interface resistance and grain-boundary scattering, respectively followed by the conclusions.

II. Theory and Computational Details

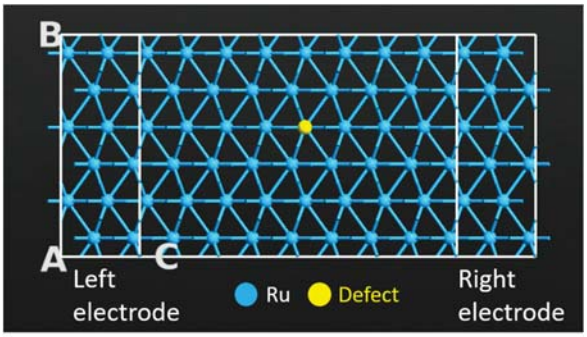

Figure 1. Two-terminal device set up used to study the change in resistivity due to defect/impurity scattering.

The scattering mechanisms in Ru interconnects are studied using the first-principles DFT simulations as implemented in the ATOMISTIX TOOLKIT (ATK) [5]–[7]. For this purpose, we construct a two probe device configuration and apply the DFT+NEGF formalism to calculate the transmission across the GB. The DFT calculations have been performed using a linear combination of double-ς pseudo-atomic orbitals (PAO's) and the local density approximation (LDA) for the exchange-correlation functional. The energy cutoff of 150 Ry

is used for the real space grid to evaluate the Kohn-Sham Hamiltonian. We used 7x7x7 Monkhorst-Pack [8] k-point grid for bulk calculations, 3x3 k-point grid for device configuration. For the electrodes in the device 5x5x401 k-point grid is used. Geometry optimizations of the GB structures have been performed using the classical potentials with threshold forces on atoms to be 0.02 eV/Å and stress tensor below 0.1 GPa. We have used Dirichelet and Neumann boundary conditions in the interface calculations for the metal and semiconductor sides, respectively. Same set of the boundary conditions are also used in the device calculations at later stage.

The recipe to determine the contact resistance is described in Ref. [9], [10] and we briefly reiterate it here. From zero-bias calculations we first calculate the transmission coefficient of the device, $T_{device}(E)$, using which the zero-bias conductance (G_{device}) can be obtained as:

$$G_{dev} = \frac{2e^2}{h}\int T_{dev}(E)(-\frac{\partial f}{\partial E})dE$$

Where, f is the Fermi-Dirac distribution. The corresponding resistance is simply $R_{dev} = 1/G_{dev}$. To calculate the GB resistance, we perform two separate calculations with GB and without GB (i.e. crystalline bulk). The GB resistance is extracted by subtracting the total resistance across the GB minus the intrinsic part of metal resistivity ($R_{GB} = R_{dev\_GB} - R_{bulk}$).

In order to project possible variation in Ru GB resistivity we use the Mayadas-Shatzkes expression:

$$\rho_{GB} = \frac{\rho_{bulk}}{1 - \frac{3}{2}\alpha + 3\alpha^2 - 3\alpha^3 \ln\left(1 + \frac{1}{\alpha}\right)}$$

Where,

$$\alpha = \frac{\lambda}{D}\frac{r}{1-r}$$

Here λ (= 8.65 nm) is the mean free path of the electron and ρ_{bulk} (= 8.8 μΩ-cm) is the bulk resistivity of Ru [11].

III. Defect Scattering

The calculated value of resistivity along the (10-10) direction is 6.87 μΩ-cm which is in excellent agreement with measured value of 7.10 μΩ-cm [12]. In order to quantify the resistivity due to impurity scattering, we perform two separate transmission calculations using the device configuration, as illustrated in Figure 2, with and without the presence of impurity and calculate the difference. In each case, the electron transmission is calculated across a central region of ~ 3 nm containing about 420 atoms in the supercell of bulk Ru along (10-10) direction. The defect concentration in the supercell is ~ $2e^{20}/cm^3$, and the defect images are well-separated by a distance of > 10Å. A k-point sampling of 3x3x101 resulting in 455 k-points was employed for transmission calculations. The results of the transmission calculations for each case are summarized in Table 1. In general, we observed that the substitutional defects leads to higher resistivity compared to the interstitial defects.

Table 1. Calculated resistivity values for four different types of defects studied.

Defect	Total resistivity (μΩ-cm)	Electrode contribution (μΩ-cm)	Defect resistance (μΩ-cm)
Vacancy	18.36	6.77	11.59
Interstitial	22.18	6.77	15.41
Carbon	22.33	6.77	15.56
Oxygen	28.31	6.77	21.54

IV. Vertical Resistance in Ru Via Structures

Next, the vertical resistance across the Ru/liner interface in typical Via structures is also calculated using the device configuration. The metal-metal interface in Via structures is important and can contribute to the MOL resistance (R_{MOL}) significantly. Here, we studied commonly used metal barriers such as Ti, TaN and TiN metal [13]. For this purpose, we construct device configuration with central region being Ru/liner interface and bulk electrodes, as illustrated in Figure 2. The transmission is calculated perpendicular to the Ru/barrier metal interface. Table 2 lists the calculated interface resistance corresponding to the Ru/metal interfaces in Via structures. The results indicate that the Ru/TiN interface has the least contact resistance and represents the best choice as liner metal.

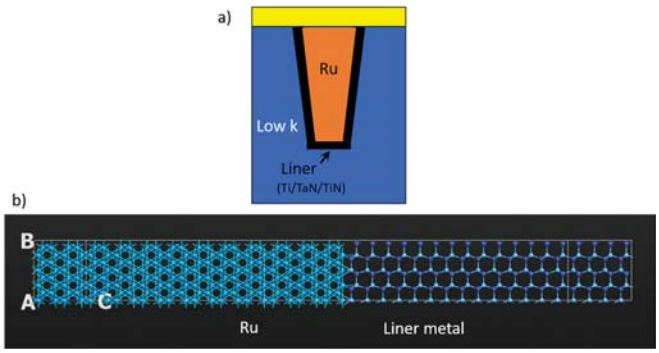

Figure 2. a) Schematic of the Via structure showing the Ru/Liner interface and b) corresponding device configuration used to calculate the interface resistance.

Table 2. Calculated area specific interface resistance for different Ru/Liner interface studied.

Liner metal	Total resistance (e^{-12} Ω-cm^2)	Electrode contribution (e^{-12} Ω-cm^2)	Interface resistance (e^{-12} Ω-cm^2)
Ti (10-10)	43.67	13.34	30.33
Ti(11-20)	89.46	16.38	73.08
TaN (10-10)	69.19	26.42	42.77
TaN (11-21)	82.30	28.66	53.64
TiN (100)	26.76	15.14	11.62
TiN (111)	22.43	16.11	30.33

V. Grain Boundary Scattering

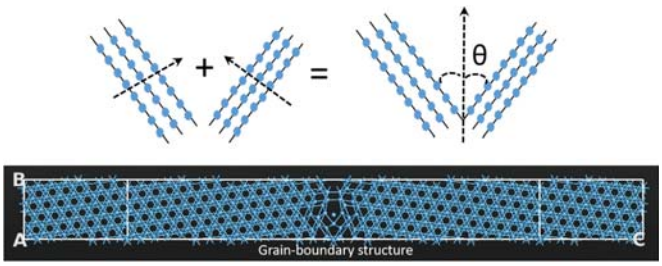

Figure 3. Construction of STGB and corresponding device structure.

A. Creating Symmstric Tilt Grain Boundries

The Symmetric Tilt Grain Boundary (STGB) structures in Ru are created using the Coincidence Site Lattice (CSL) scheme [14]. First a surface from bulk Ru crystal is cleaved along the chosen crystallographic direction and a mirrored copy it are joined together to form a grain boundary. This is called STGB corresponding to the surface under consideration, as illustrated in Figure 3. In order to maintain the periodic boundary conditions, we choose the surface cell large enough (along the z-direction) that prevents any spurious interactions between the two parallel boundaries and other finite-size artifacts. Typically, GB constructed with this approach contains few hundreds of atoms in the simulation box.

B. Optimizing the Grain Boundary structures

The GB structures created using above mentioned scheme needs to be optimized to reduce the forces acting on the atoms due to lattice mismatch at the interface of the two grains. For this purpose, we create a device configuration as shown in Figure 3. The device configuration consists of left and right electrode, which essentially are the periodic bulk-like extensions of the two Ru grains, and a central region which essentially contain the GB structure. In this device configuration we relax the forces acting on all the atoms at the interface, using the classical embedded atom (EAM) potentials [5], below threshold value of 0.001eV/Å. The optimized device configuration is then used to evaluate the transmission spectrum across the Ru GB.

C. Reflection coefficients across Grain Boundary

The calculated reflection coefficients across the symmetric tilt GB's are 0.48, 0.45, 0.51, 0.50 and 0.38 for Σ3, Σ7, Σ13, Σ19, and Σ49, respectively. A wide range of grain angles between low (13.44°) to high (86.63°) are considered for calculation of the reflection coefficients. The calculated reflection coefficients vary between 0.38 up to 0.51. We further use the Mayadas-Shatzkes expression to evaluate the variation in the metal resistivity as a function of grain diameter. The projected values of the resistivities are shown in Figure 4. The red dots in this graph corresponds to measure hardware data in the experiments [4]. The blue and green curves corresponds to the projected resistivities for the minimum and maximum reflection coefficient observed for STGB structures.

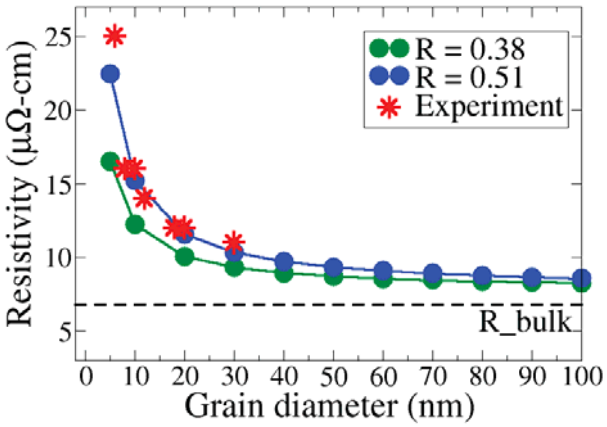

Figure 4. Resistivity scaling of Ru GB's using the Mayadas-Shatzkes expression for R=0.38 and R=0.51.

VI. Conclusions

In conclusion, we have reported a comprehensive study of scattering mechanism for Ru interconnects. Our results show that the defects and impurities can change the Ru resistivity by an order of magnitude. Among three liner metals TiN appears to be the most suitable choice owing to the minimal contact resistance. We also studied STGB's in Ru and the calculated reflection coefficients vary from 0.38 to 0.51. Our results are in good agreement with the experimentally reported value. Further, using Mayadas-Shatzkes model, we predict the possible enhancement of the metal resistivity due to the GB scattering. A reflection coefficient of 0.51 provides best fit for experimental data. Our study thus provide a deeper understanding of the GB resistivity in polycrystalline Ru and have implications towards engineering the metal interconnect resistance in modern IC's.

References

[1] L. G. Wen *et al.*, "Ruthenium metallization for advanced interconnects," in *2016 IEEE International Interconnect Technology Conference / Advanced Metallization Conference (IITC/AMC)*, 2016, pp. 34–36.

[2] N. Jourdan *et al.*, "CVD-Mn/CVD-Ru-based barrier/liner solution for advanced BEOL Cu/Low-k interconnects," in *2016 IEEE International Interconnect Technology Conference / Advanced Metallization Conference (IITC/AMC)*, 2016, pp. 37–39.

[3] X. Zhang *et al.*, "Ruthenium interconnect resistivity and reliability at 48 nm pitch," in *2016 IEEE International Interconnect Technology Conference / Advanced Metallization Conference (IITC/AMC)*, 2016, pp. 31–33.

[4] S. Dutta *et al.*, "Ruthenium interconnects with 58 nm2 cross-section area using a metal-spacer process," in *2017 IEEE International Interconnect Technology Conference (IITC)*, 2017, pp. 1–3.

[5] "Home." [Online]. Available: https://quantumwise.com/. [Accessed: 02-Apr-2018].

[6] J. M. Soler *et al.*, “The SIESTA method for ab initio order- N materials simulation,” *J. Phys. Condens. Matter*, vol. 14, no. 11, p. 2745, 2002.
[7] M. Brandbyge, J.-L. Mozos, P. Ordejón, J. Taylor, and K. Stokbro, “Density-functional method for nonequilibrium electron transport,” *Phys. Rev. B*, vol. 65, no. 16, p. 165401, Mar. 2002.
[8] H. J. Monkhorst and J. D. Pack, “Special points for Brillouin-zone integrations,” *Phys. Rev. B*, vol. 13, no. 12, pp. 5188–5192, Jun. 1976.
[9] T. Markussen and K. Stokbro, “Metal-InGaAs contact resistance calculations from first principles,” in *2016 International Conference on Simulation of Semiconductor Processes and Devices (SISPAD)*, 2016, pp. 373–376.
[10] H. Dixit *et al.*, “First-Principles Investigations of TiGe/Ge Interface and Recipes to Reduce the Contact Resistance,” *IEEE Trans. Electron Devices*, vol. 64, no. 9, pp. 3775–3780, Sep. 2017.
[11] D. Gall, “Electron mean free path in elemental metals,” *J. Appl. Phys.*, vol. 119, no. 8, p. 085101, Feb. 2016.
[12] S. Kasap, C. Koughia, and H. E. Ruda, “Electrical Conduction in Metals and Semiconductors,” in *Springer Handbook of Electronic and Photonic Materials*, Springer, Cham, 2017, pp. 1–1.
[13] S. Dey *et al.*, “Atomic layer deposited ultrathin metal nitride barrier layers for ruthenium interconnect applications,” *J. Vac. Sci. Technol. Vac. Surf. Films*, vol. 35, no. 3, p. 03E109, Apr. 2017.
[14] D. H. Warrington and P. Bufalini, “The coincidence site lattice and grain boundaries,” *Scr. Metall.*, vol. 5, no. 9, pp. 771–776, Sep. 1971.